Hindawi Publishing Corporation
Journal of Nanomaterials
Volume 2013, Article ID 690180, 7 pages
http://dx.doi.org/10.1155/2013/690180

Research Article

Effect of Structure, Composition, and Micromorphology on the Hydrophobic Property of F-DLC Film

Aihua Jiang,[1,2] Jianrong Xiao,[2,3] Xinyu Li,[2] and Zhiyong Wang[2]

[1] *Guangxi Scientific Experiment Center of Mining, Metallurgy and Environment, Guilin University of Technology, Guilin 541004, China*
[2] *College of Science, Guilin University of Technology, Guilin 541004, China*
[3] *Guangxi Key Laboratory of Information Materials, Guilin University of Electronic Technology, Guilin 541004, China*

Correspondence should be addressed to Jianrong Xiao; xjr@glut.edu.cn

Received 26 June 2013; Revised 13 September 2013; Accepted 15 September 2013

Academic Editor: Lavinia Balan

Copyright © 2013 Aihua Jiang et al. This is an open access article distributed under the Creative Commons Attribution License, which permits unrestricted use, distribution, and reproduction in any medium, provided the original work is properly cited.

Fluorinated diamond-like carbon (F-DLC) films were prepared by radio frequency plasma-enhanced chemical vapor deposition technique with CF_4 and CH_4 as source gases under different deposition conditions. The chemical bonding structure and composition of the films were detected by Raman, Fourier transform infrared absorption spectrometry (FTIR), and X-ray photoelectron spectroscopy (XPS) characterization. The micromorphology and surface roughness of the film were observed and analyzed by atomic force microscopy (AFM). The results indicated that all the prepared films presented a diamond-like carbon structure. The relative content of fluorine in the films increased, containing more CF_2 groups. The ratio of hybrid structure sp^3/sp^2 decreased. The surface roughness of the films increased when the gas flow ratio R ($R = CF_4/[CH_4 + CF_4]$) or the deposition power increased. The contact angle of water with the surface of the F-DLC film was measured with a static drop-contact angle/surface tension measuring instrument. The hydrophobic property of the F-DLC films was found to be dependent on the sp^2 structure, fluorine content, and surface roughness of the films. The contact angle increased when the relative content of fluorine in the films and sp^2 content increased, whereas the contact angle first increased and then decreased with the surface roughness.

1. Introduction

In recent years, fluorinated amorphous carbon film (a-C:F) has attracted the attention of researchers for its application as a film with a low dielectric constant [1–3], a self-lubricating and low friction resistance film [4, 5], an antireflection film with low refractive index and small dispersion, or a protective film against strong ultraviolet absorption [6, 7]. Carbon atoms form chemical bonds via three different hybridizations, namely, sp^1, sp^2, and sp^3, in amorphous carbon, including diamond-like carbon (DLC) film, graphite-like carbon (GLC) film, and polymer-like carbon (PLC) film. Fluorinated DLC (F-DLC) film is a new fluorinated amorphous carbon material that combines the properties of both the DLC film and the a-C:F film, and this material has a broad application prospect [8–13]. The sp^1 content in the F-DLC film is very low. Therefore, the properties of the film mainly depend on the relative content of sp^3 bonding of DLC and sp^2 bonding of GLC. Compared with DLC films, the physical properties of the films are changed by the introduction of strongly electronegative fluorine due to their compositions and chemical bonding structures. Many researchers focus on the electronic and optical properties of F-DLC films. However, existing studies rarely dealt with other characteristics of F-DLC films (e.g., hydrophobicity, biological compatibility), which are expected to be applicable in the field of medicine [14–17]. An F-DLC film and polytetrafluoroethylene (PTFE) are very much alike in terms of their hydrophobic property, as both have a $C\text{-}F_2$ group. The poor mechanical properties of PTFE and its loose combination with the substrate limit its application under certain conditions (e.g., surgical scalpel, heart stent) [18, 19]. F-DLC films have consequently become

a new area of research interest because of their good biocompatibility, antibacterial adhesion, mechanical properties, and hydrophobic properties.

This paper investigated the relationship among the chemical bonding structure, composition, surface morphology, and hydrophobic properties of F-DLC films prepared under different gas flow ratios R ($R = CF_4/[CH_4 + CF_4]$). The findings of this research are of significant reference value for F-DLC films applied in clinical medicine.

2. Experimental

2.1. Preparation of F-DLC Films. The radio frequency plasma-enhanced chemical vapor deposition (PECVD) equipment used in the experiment was designed and developed by Shenyang Scientific Instruments Co., Ltd. at the Chinese Academy of Sciences. CF_4 and CH_4 were used as source gases, whereas Ar was used as a working gas. The total gas flow was 45 sccm, whereas that of Ar was kept at 5 sccm. The deposition temperature was 100°C, whereas the deposition power and gas flow ratio R ($R = CF_4/[CH_4 + CF_4]$) were changed. The total gas pressure was controlled at approximately 5.5 Pa during the experimental process. Monocrystal silicon (100) surface used as substrate was soaked and ultrasonically cleaned in acetone, alcohol, and deionized water for 20 min to remove organic contamination and natural oxidation layers from the surface. The background pressure was 1.0×10^{-3} Pa. Prior to deposition, the substrate surface was first bombarded for 15 min at a power of 100 w in an Ar atmosphere.

2.2. Structure, Composition, and Micromorphological Characterization of F-DLC Films. Raman is a common technique that uses a Raman spectrum to characterize and detect the sp hybrids of carbon-based material. In this paper, the scattering spectra of the films prepared under different flow ratios were tested by Dilor LabRam Infinity (the wavelength of the laser is 632.8 nm), and the relative content of sp hybridizations in the films was detected. The chemical bonding structure of the films was analyzed with a Fourier transform infrared absorption spectrometry (FTIR; NEXUS470). The surface structures of the films were performed to characterize by an X-ray photoelectron spectroscopy (XPS, Microlab 310-F). Variations in micromorphology and surface roughness of the films under different flow ratios were observed by an atomic force microscopy (AFM; SOLVER P47).

2.3. Surface Energy Analysis and Contact Angle Measurement of the Films. The contact angle between a liquid and a solid surface is a manifestation of hydrophobic property. The size of the contact angle is determined by the surface free energy. The interfacial total energy remains constant when the interface between liquid and solid is stable, that is, satisfying Young's equation [16]:

$$r_{sv} = r_{sl} + r\cos\theta_e, \tag{1}$$

where r_{sv} and r_{sl} are the surface energy of the solid and liquid, respectively, r is the interfacial tension between the solid and liquid, and θ_e is the contact angle. The contact angle of a liquid and a solid can be large or zero (complete wetting) because of the strong polarization of a solid. The above equation expressed in terms of polarization has the following form:

$$\cos\theta_e = \frac{2a_s}{a_l} - 1, \tag{2}$$

where a_s and a_l are the polarization of the solid and liquid, respectively. The contact angle with polar liquid molecules increases as the surface free energy decreases. The contact angle between water and the film was measured by a JC2000C3 static drop-contact angle/surface tension measuring instrument.

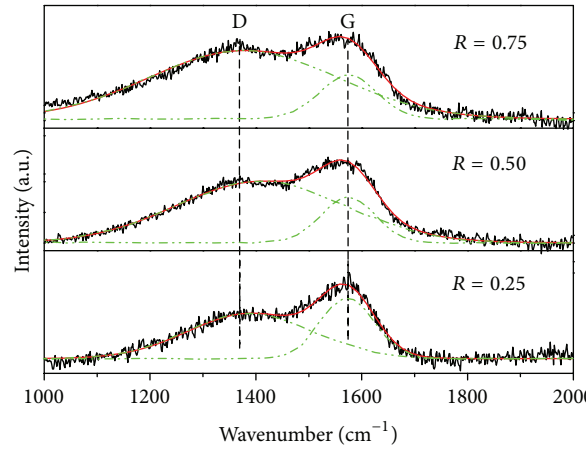

Figure 1: Raman spectra of the F-DLC films prepared with various values of R.

3. Results and Discussion

3.1. Chemical Bonding Structure and Composition of the Films. Figure 1 is the Raman spectrum of the F-DLC films deposited under different R (deposition power 100 w). The R values are 0.25, 0.5, and 0.75, and the corresponding thicknesses of the films are 96.7 nm, 101.8 nm, and 104.5 nm, respectively. The presence of peaks D and G demonstrates that all the prepared films had diamond-like carbon structures. Lorentzian fitting was performed by resolving the spectrum into peaks to study the effect of R on hybrid structure sp in films. The band positions ω_D and ω_G of peaks D and G, as well as the integrated intensity ratios of two peaks I_D/I_G for each spectral line, are listed in Table 1. The position of peak G is relatively stable, whereas peak D shifts toward a higher frequency under different R. According to the model of Beeman et al. [20], the information on bond angle disorder and bonding structure is contained in the peak position. Bond angle disorder and a certain number of coordination bonds result in the shifting toward a lower frequency of peaks G and D. The shift toward a higher frequency on the Raman spectrum indicates that the bond angle disorder is eliminated to some extent. The value of I_D/I_G gradually increasing with R is known. The increasing I_D/I_G indicates that the sp^2 content of

Table 1: Variation of peak position, width, and I_D/I_G ratio obtained by Raman spectroscopy.

Gas flow ratio R	D band		G band		I_D/I_G
	Position ω_D (cm^{-1})	Width	Position ω_G (cm^{-1})	Width	
0.25	1389.6	251.7	1572.5	102.8	1.70
0.50	1401.8	318.4	1574.5	101.5	4.19
0.75	1407.1	356.3	1574.6	107.7	5.17

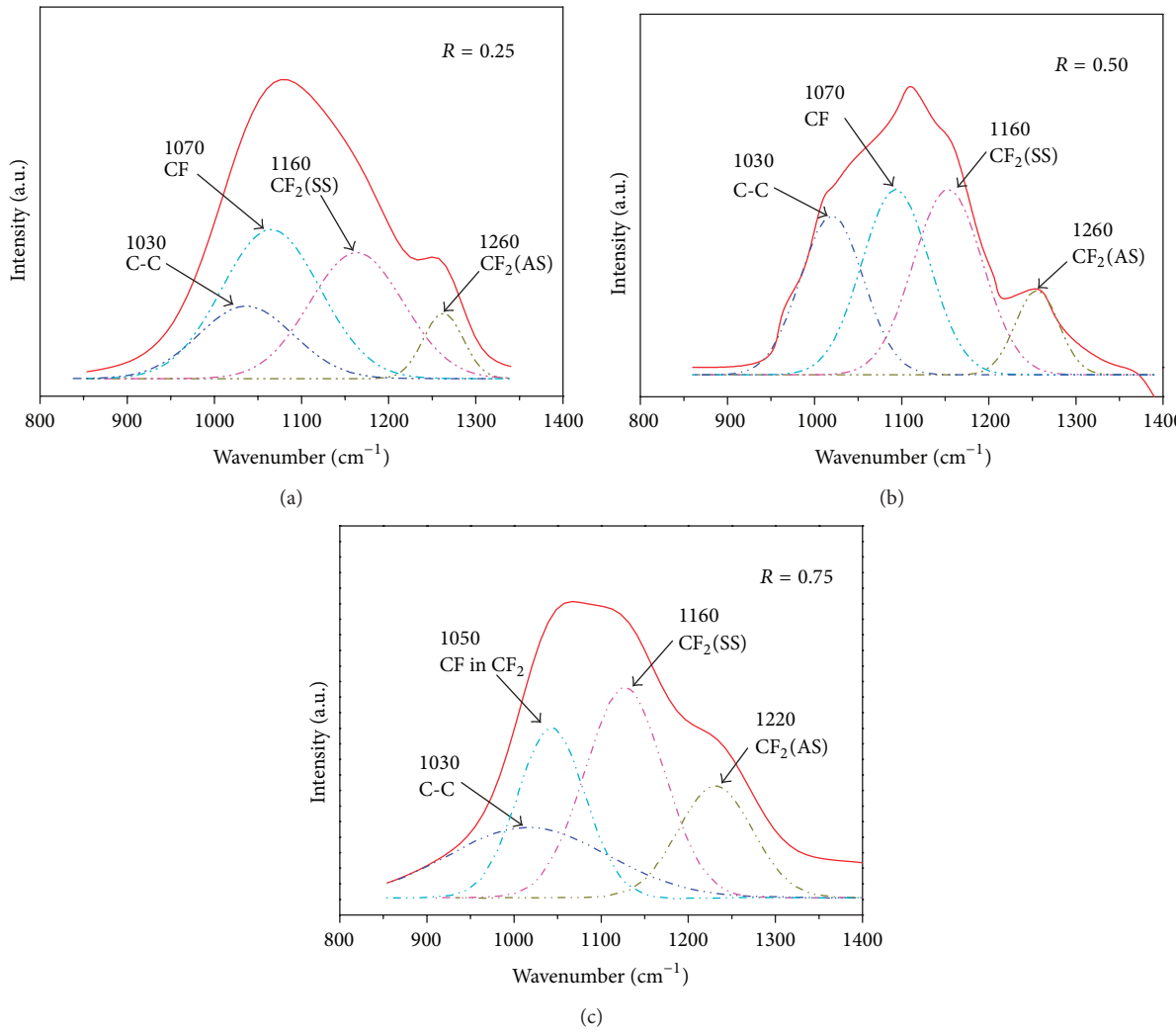

Figure 2: FTIR spectra of the F-DLC films prepared with various values of R (deposition power 100 w).

bonded carbon increased in the film and that graphitization occurred in accordance with the reverse correlation of sp^3/sp^2 and I_D/I_G [21, 22].

The FTIR absorption peaks of the diamond-like structure had a wave number of 900 cm^{-1} to 1400 cm^{-1}. For the main absorption peaks, 1030, 1070, 1160, and 1260 cm^{-1} corresponded to the C-C, CF, CF_2(SS), and CF_2(AS) absorption peaks, respectively [7, 23, 24]. The FTIR spectra (900 cm^{-1} to 1400 cm^{-1} range) of the F-DLC films deposited under different R are shown in Figure 2. The shape of three curves varied greatly by changing the R, indicating that the effect of R on the structure and composition of the film was significant. The Gaussian fitting of the infrared spectra revealed that the C-C absorption peaks gradually weakened, whereas CF_2 absorption peaks were enhanced slightly. CF absorption peaks were significantly enhanced as R increased. In this process, the mesh structure of carbon in the film was partly fractured with the increase of R, with some carbon atoms being substituted by fluorine atoms. Thus, fluorine ions were effectively incorporated into the film. Generally, the C-F_x ($x = 1, 2$) vibration peak of the film on the FTIR spectra exhibited a shift toward a higher frequency as the R increased. This relationship may be attributed to the many fluorine-containing groups in plasma participating in the

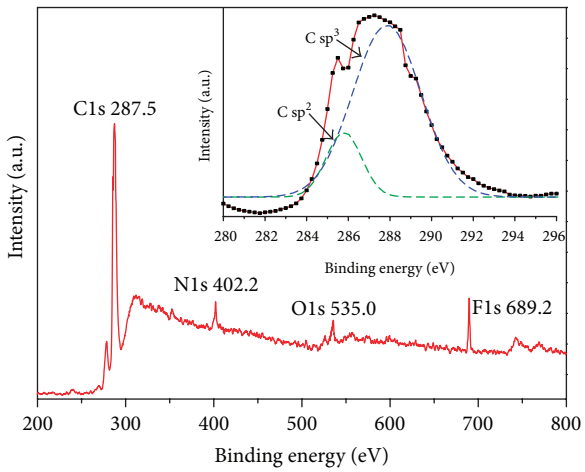

Figure 3: Typical XPS spectrum of the films. Illustration: deconvolution of the XPS C1s peaks of the films.

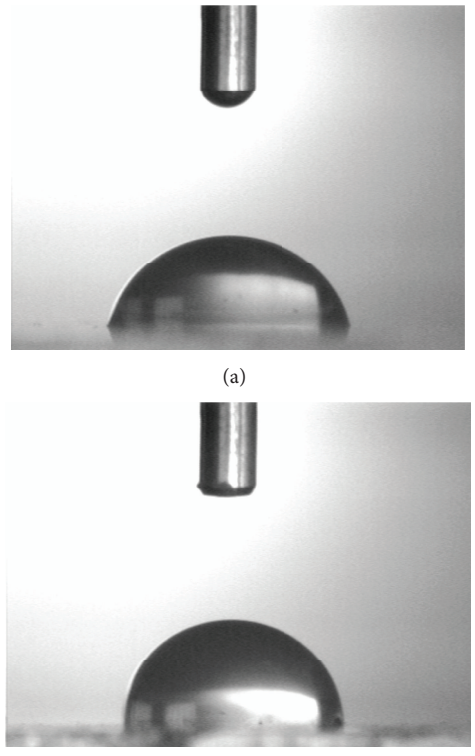

(a)

(b)

Figure 4: Liquid droplet on the surface of DLC films before and after F doped: (a) DLC films; (b) F-DLC films.

deposition of the film in the vacuum chamber when R increased, resulting in an increase of fluorine content. As the concentration of strongly electronegative fluorine atoms in the film increased, the vibration peaks shifted toward a higher frequency. The relative concentration of F atom in the film can simultaneously be estimated according to FTIR spectral lines and to the following Beer equation [10, 24]:

$$n_x = A \int \frac{\alpha(\omega)}{\omega} d\omega, \quad (3)$$

where n_x is the atomic relative concentration of F, $\alpha(\omega)$ is the absorption coefficient at ω, and A is constant.

Figure 3 shows the typical XPS spectrum for the films deposited at $R = 0.5$. The peaks of the XPS spectrum at 287.5 eV, 402.2 eV, 535.0 eV, and 689.2 eV can be due to the photoelectrons exited from the C1s, N1s, O1s, and F1s levels, respectively [25]. The O1s peak in the films may come from the H_2O in the vacuum chamber before deposition. The illustration of Figure 3 shows the Gaussian fitting analysis curves of C1s peaks. The C1s peak was assumed to consist of two peaks, the sp^3 peak and sp^2 peak [25], and we can obtain the values of the sp^3/sp^2.

3.2. Hydrophobic Property of the Films. The contact angles of water with the DLC film surface before and after fluorine doping are presented in Figure 4. The contact angle clearly increased after fluorine doping in the DLC film. Thus, the hydrophobic property significantly improved.

Figure 5 shows the surface roughness of the films as a function of the gas flow ratio. With increasing gas flow ratio, the surface roughness of the films increases from 1.93 to 2.02, and this shows that the gas flow ratio has little effect on the surface roughness of the films. The hydrophobic property of the F-DLC film is affected by chemical bonding structure and composition. The changes of the contact angle with R are plotted in Figure 6. The contact angle largely depended on the change of R. The contact angle sharply increased with R when the value of R was less than 0.75. However, the increase rate of the contact angle slowed down when R was greater than 0.75. The curve b in Figure 6 represents the relationship between the contact angle of water with the F-DLC film and the change of relative fluorine content in the film. We can see that the contact angle rapidly increased first and then gradually rose as the concentration of fluorine increased. Given the presence of CF and CF_2, which are main groups that affect the hydrophobic property of the film, the increase of fluorine content per unit volume caused the fluorine atoms to migrate because of the small interactions between fluorine atoms. Thus, the fluorine atoms easily concentrated on the surface, leading to the rapid decline of surface energy. In addition, the surface energy of the compounds formed by CF_x was far lesser than that of the water. The lower the surface free energy of the materials was, the higher the hydrophobic property of the film and the greater the contact angle became. Therefore, the contents of CF and CF_2 increased and the surface energy decreased with improved hydrophobic property and a higher contact angle as the R increased. On the other hand, I_D/I_G increased with R increasing, and sp^3/sp^2 ratio decreased. The graphite content sp^2 hybridized relative increased. The typical three-dimensional diamond-like films transformed into two-dimensional polymeric structure. The polarity of the films decreased, and polarization intensity decreased. It leads to the film easily by water infiltration, and the contact angle becomes large.

The mechanism behind the lotus effect is the cells on lotus leaf surface having a micro-/nanodual-scale structure of papillae and the surface microstructure containing hydrophobic wax resinite [26]. Therefore, from the bionic

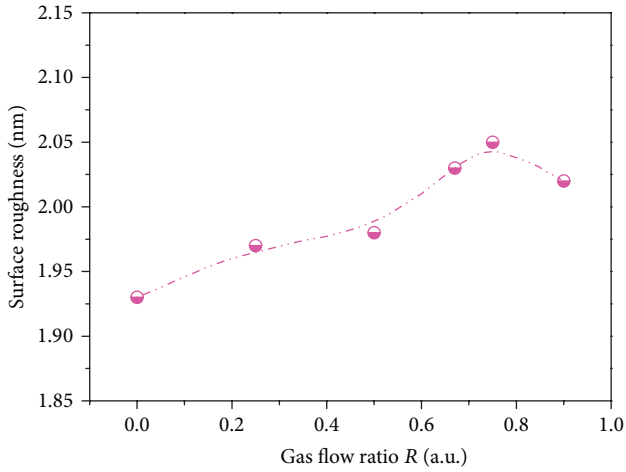

FIGURE 5: Surface roughness of the films as a function of gas flow ratio R.

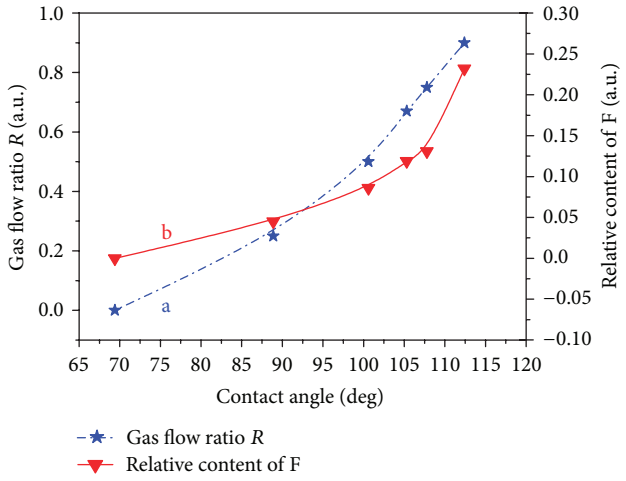

FIGURE 6: Variation of contact of the F-DLC films at various (a) gas flow ratios R and (b) relative contents of F.

point of view, changing the surface roughness of the film can improve its hydrophobic property. Figure 7 shows the AFM micrographs under different deposition powers when $R = 0.75$, from which the surface roughness of the film can be obtained. The thickness of the films deposited under 100 w and 250 w is 104.5 nm and 181.6 nm, respectively. The curves of deposition power plotted against surface roughness and contact angle are given in Figure 8. The contact angle of water with the film surface first increased and then decreased to some extent. Furthermore, the contact angle reached the maximum 110.3° when the deposition power was 100 w. The reason for such variation pattern is that the film deposited had a smoother surface at a low deposition power and that the film surface presented a micro-/nanodual-scale when the deposition power was approximately 100 w. When the deposition power continued to increase, the etching of grains on the film surface increased as well, thereby causing a micro-/nanodual-scale change. Some projection packets appear on the film surface. As a result, the surface became

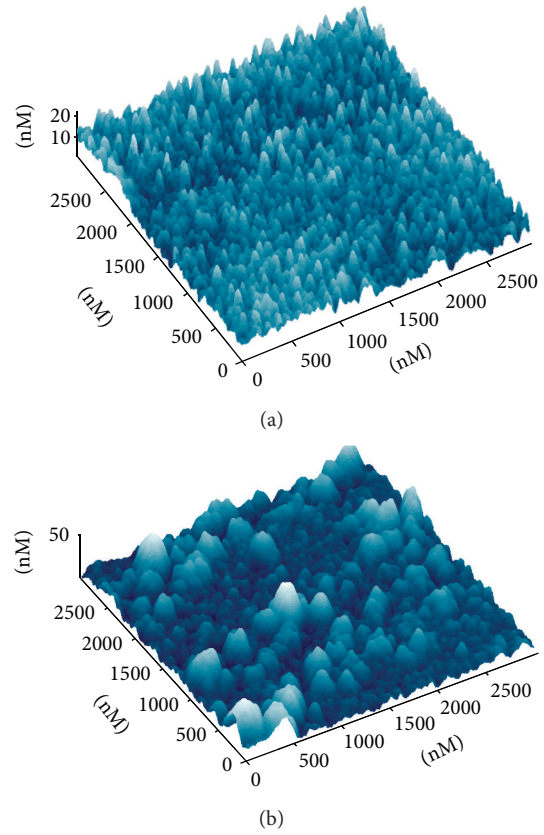

FIGURE 7: AFM 3D image of F-DLC films prepared at (a) 100 w and (b) 250 w.

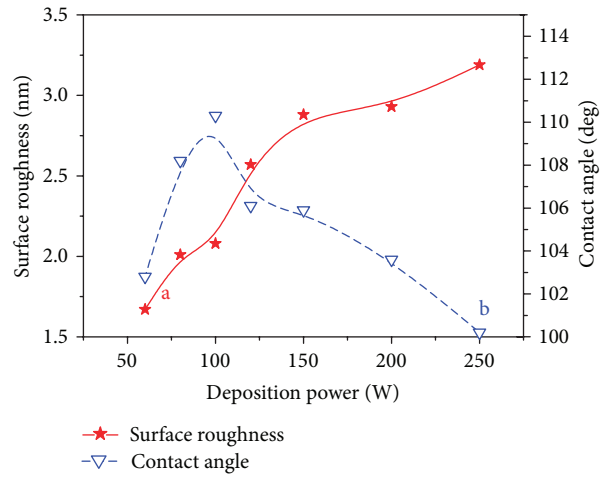

FIGURE 8: Curve (a): surface roughness as a function of deposition power. Curve (b): contact angle as a function of deposition power.

rougher and contained more defects, and the contact angle decreased.

4. Conclusion

The hydrophobic properties of F-DLC films mainly depend on the chemical bonding structure of the film surface, the

fluorine content in the film, polarization, and the surface roughness of the film. The content of weakly polarized radical CF_2 increased with the increase of R, and the fluorine content in the films increased. Thus, the surface energy decreased and polarization was reduced. The resulting higher contact angle between the F-DLC film and water and the higher content of sp^2 indicated that wetting worsened. In the preparation process, the contact angle increased with an increasing gas flow ratio; the surface roughness increased, whereas the contact angle first increased and then slightly decreased as the deposition power increased.

Acknowledgments

This work was supported by the National Science Foundation of China (Grant nos. 11064003 and 11364011), the Guangxi Natural Science Foundation (Grant no. 2010GXNSFA013122), and the Research Funds of the Guangxi Key Laboratory of Information Materials (Grant no. 0710908-06-K). The authors also genuinely thank Ph.D. Yanwei Li for his help in the technical and language checking.

References

[1] H. J. Ahn, J. B. Kim, B. H. Hwang, H. K. Baik, J. S. Park, and D. Kang, "Structural and chemical characterization of fluorinated amorphous carbon films (a-C:F) as a liquid crystal alignment layer," *Diamond and Related Materials*, vol. 17, no. 12, pp. 2019–2024, 2008.

[2] H. Yokomichi and A. Masuda, "Effect of sputtering with hydrogen dilution on fluorine concentration of low hydrogen content fluorinated amorphous carbon thin films with low dielectric constant," *Journal of Applied Physics*, vol. 86, no. 5, pp. 2468–2472, 1999.

[3] S. F. Ahmed, D. Banerjee, and K. K. Chattopadhyay, "The influence of fluorine doping on the optical properties of diamond-like carbon thin films," *Vacuum*, vol. 84, no. 6, pp. 837–842, 2010.

[4] M. Rubio-Roy, C. Corbella, E. Bertran et al., "Effects of environmental conditions on fluorinated diamond-like carbon tribology," *Diamond and Related Materials*, vol. 18, no. 5–8, pp. 923–926, 2009.

[5] Z. Q. Yao, P. Yang, N. Huang, H. Sun, and J. Wang, "Structural, mechanical and hydrophobic properties of fluorine-doped diamond-like carbon films synthesized by plasma immersion ion implantation and deposition (PIII-D)," *Applied Surface Science*, vol. 230, no. 1–4, pp. 172–178, 2004.

[6] X. Wang, H. R. Harris, K. Bouldin et al., "Structural properties of fluorinated amorphous carbon films," *Journal of Applied Physics*, vol. 87, no. 1, pp. 621–623, 2000.

[7] J. W. Yi, Y. H. Lee, and B. Farouk, "Annealing effects on structural and electrical properties of fluorinated amorphous carbon films deposited by plasma enhanced chemical vapor deposition," *Thin Solid Films*, vol. 423, no. 1, pp. 97–102, 2003.

[8] Y. Haruyama, Y. Kang, M. Okada, and S. Matsui, "Electronic structure of fluorinated diamond-like carbon thin films as a function of annealing temperature using photoelectron spectroscopy," *Journal of Electron Spectroscopy and Related Phenomena*, vol. 184, no. 3–6, pp. 276–279, 2011.

[9] M. Kawaguchi, J. Choi, and T. Kato, "Vapor deposition of perfluoropolyether lubricant on fluorinated diamondlike carbon surface," *Journal of Applied Physics*, vol. 99, Article ID 08N108, 3 pages, 2006.

[10] J. R. Xiao and A. H. Jiang, "Effect of radio frequency power on the structural and optical properties of nitrogen doping of fluorinated diamond-like carbon thin films," *Journal of Physics D*, vol. 41, pp. 225304–222538, 2008.

[11] F. R. Marciano, D. A. Lima-Oliveira, N. S. Da-Silva, E. J. Corat, and V. J. Trava-Airoldi, "Antibacterial activity of fluorinated diamond-like carbon films produced by PECVD," *Surface and Coatings Technology*, vol. 204, no. 18-19, pp. 2986–2990, 2010.

[12] N. Yamada, K.-I. Nakamatsu, K. Kanda, Y. Haruyama, and S. Matsui, "Surface evaluation of fluorinated diamond-like carbon thin film as an antisticking layer of nanoimprint mold," *Japanese Journal of Applied Physics*, vol. 46, no. 9 B, pp. 6373–6374, 2007.

[13] K.-I. Nakamatsu, N. Yamada, K. Kanda, Y. Haruyama, and S. Matsui, "Fluorinated diamond-like carbon coating as antisticking layer on nanoimprint mold," *Japanese Journal of Applied Physics*, vol. 45, no. 33-36, pp. L954–L956, 2006.

[14] T. Saito, T. Hasebe, S. Yohena et al., "Antithrombogenicity of fluorinated diamond-like carbon films," *Diamond and Related Materials*, vol. 14, no. 3-7, pp. 1116–1119, 2005.

[15] Y. H. Lin, Y. C. Syue, H. D. Lin et al., "Fluorinated DLC deposited by pulsed-DC plasma for antisticking surface applications," *Diamond and Related Materials*, vol. 17, pp. 1728–1732, 2008.

[16] J. S. Chen, S. P. Lau, Z. Sun et al., "Metal-containing amorphous carbon films for hydrophobic application," *Thin Solid Films*, vol. 398-399, pp. 110–115, 2001.

[17] G. Chen, J. Zhang, and S. Yang, "Fabrication of hydrophobic fluorinated amorphous carbon thin films by an electrochemical route," *Electrochemistry Communications*, vol. 10, no. 1, pp. 7–11, 2008.

[18] K. Ozeki, I. Nagashima, K. K. Hirakuri, and T. Masuzawa, "Adsorptive properties of albumin, fibrinogen, and γ-globulin on fluorinated diamond-like carbon films coated on PTFE," *Journal of Materials Science*, vol. 21, no. 5, pp. 1641–1648, 2010.

[19] J. A. McLaughlin, B. Meenan, P. Maguire, and N. Jamieson, "Properties of diamond like carbon thin film coatings on stainless steel medical guidewires," *Diamond and Related Materials*, vol. 5, no. 3–5, pp. 486–491, 1996.

[20] D. Beeman, J. Silverman, R. Lynds, and M. R. Anderson, "Modeling studies of amorphous carbon," *Physical Review B*, vol. 30, no. 2, pp. 870–875, 1984.

[21] H.-S. Jung and H.-H. Park, "Structural and electrical properties of co-sputtered fluorinated amorphous carbon film," *Thin Solid Films*, vol. 420-421, pp. 248–252, 2002.

[22] A. C. Ferrari and J. Robertson, "Interpretation of Raman spectra of disordered and amorphous carbon," *Physical Review B*, vol. 61, no. 20, pp. 14095–14107, 2000.

[23] A. J. M. Buuron, M. C. M. Van De Sanden, W. J. Van Ooij, R. M. A. Driessens, and D. C. Schram, "Fast deposition of amorphous carbon films by an expanding cascaded arc plasma jet," *Journal of Applied Physics*, vol. 78, no. 1, pp. 528–540, 1995.

[24] S. Liu, S. Gangopadhyay, G. Sreenivas, S. S. Ang, and H. A. Naseem, "Infrared studies of hydrogenated amorphous carbon (a-C:H) and its alloys (a-C:H,N,F)," *Physical Review B*, vol. 55, no. 19, pp. 13020–13024, 1997.

[25] T. Y. Leung, W. F. Man, P. K. Lim, W. C. Chan, F. Gaspari, and S. Zukotynski, "Determination of the sp3/sp2 ratio of a-C:H by XPS and XAES," *Journal of Non-Crystalline Solids*, vol. 254, no. 1–3, pp. 156–160, 1999.

[26] P. Ball, "Shark skin and other solutions," *Nature*, vol. 400, no. 6744, pp. 507–509, 1999.

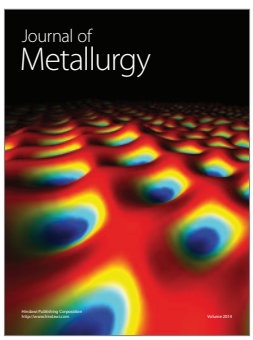

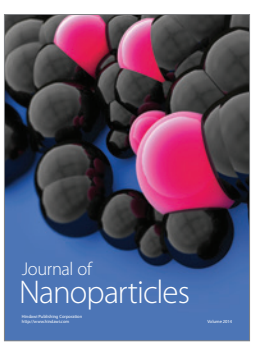

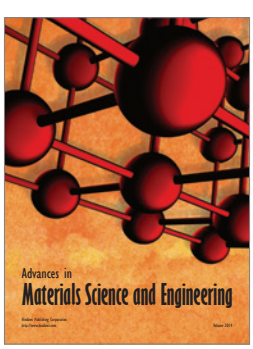

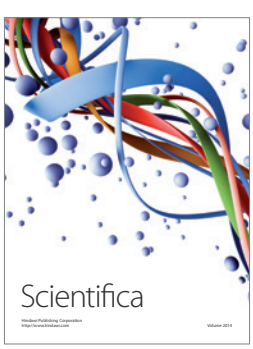

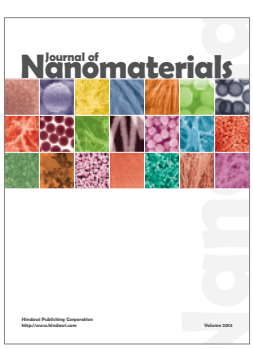

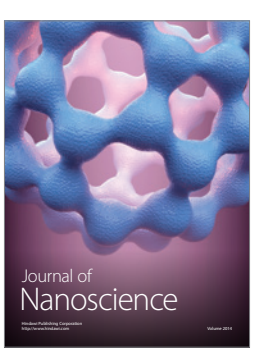

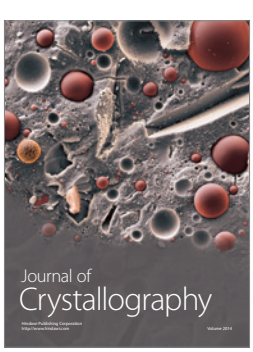

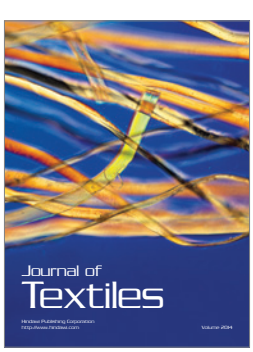

Hindawi

Submit your manuscripts at
http://www.hindawi.com